Interpreting the softening of nanomaterials through gradient plasticity

Xu Zhang
School of Civil Engineering and Mechanics, Huazhong University of Science and Technology, Wuhan 430074, China; and Laboratory of Mechanics and Materials, Aristotle University of Thessaloniki, Thessaloniki 54124, Greece

Katerina E. Aifantis[a)]
Laboratory of Mechanics and Materials, Aristotle University of Thessaloniki, Thessaloniki 54124, Greece; and Physics Department, Michigan Technological University, Houghton, Michigan 49931

(Received 4 February 2011; accepted 1 April 2011)

Experimental and simulation studies have shown that decreasing the grain size below a critical value results in softening rather than hardening in both the yield stress and flow stress of nanomaterials. In this work, a gradient plasticity framework is presented that can capture this softening behavior by treating grain boundaries as a separate phase with a finite thickness. The theoretical expression obtained for the yield stress as a function of the grain size can capture numerous experimental data that exhibit this "normal" to "abnormal" Hall–Petch transition, and an analytical equation is obtained that can predict the grain size at which this transition occurs. Furthermore, analytical expressions are obtained for the flow stress in nanomaterials, and they are in precise agreement with atomistic simulations on nanocrystalline Cu, which predict that below a critical grain size the flow stress decreases proportional to it.

I. INTRODUCTION

It is well known that the famous Hall–Petch (H–P) equation can be generally used for modeling the dependence of the yield stress on the grain size of traditional polycrystalline materials. Over the past decade, however, it has been documented that as the grain size (d) is reduced to the nanometer regime, an inverse H–P behavior is observed. In other words, there is a critical nanograin size (d_{cr}) where a "transition" occurs from hardening ($d > d_{cr}$) to softening ($d < d_{cr}$) behavior. There exist numerous experimental studies that document this hardening-to-softening behavior,[1–8] and they all attribute it to the change in deformation mechanisms below a critical grain size due to grain boundary (GB) effects. Recently, further experiments have shown that such softening is also observed for nanotwinned Cu when the twin thickness is below 15 nm.[9]

Two main theoretical approaches have been followed in trying to interpret this "anomalous" H–P behavior for nanomaterials. One is based on dislocation mechanisms and associated changes as the grain size crosses over from the microcrystalline to the nanocrystalline regime. The other approach is based on geometry and the rule of mixtures by viewing the polycrystal as a superposition of "bulk" and "GB" material. Relevant references for both approaches can be found in Refs. 10–12 and references therein, as well as in the initial articles[13,14] where some background ideas related to this article are also used.

A third most recent approach has also been introduced that combines the aforementioned two as follows: (i) an interface energy term is introduced which depends on dislocation mechanisms at the interface and allows the interface to follow its own yield behavior and (ii) a boundary layer is considered which yields along with the GB while the grain interior (GI) remains elastic.[15,16] This third approach, therefore, is a compromise of the first two since: (i) it distinguishes between "bulk" and "GB" behavior, by allowing the GB to follow its own plastic behavior through the introduction of an interface energy term and (ii) it accounts for a variety of underlying dislocation mechanisms by allowing for the development of strain gradients across the grain–GB interface.

Although the aforementioned underlying physical mechanisms of deformation are consistent with what occurs at the nanoscale, the theoretical approach[15,16] was based on a gradient plasticity model with an interface energy term that was developed for considering interfaces at the micronscale,[17] which allow for dislocation pileups.

A limitation, hence, in applying the interface gradient plasticity works[15,16] at the nanoscale, is that the GB was treated as a surface, rather than allowing it to have a finite thickness, which is the case for nanocrystals; furthermore, the interface energy was introduced phenomenologically,

a)Address all correspondence to this author.
e-mail: k.aifantis@mom.gen.auth.gr
DOI: 10.1557/jmr.2011.123

 © Materials Research Society 2011

https://doi.org/10.1557/jmr.2011.123 Published online by Cambridge University Press

rather than being related to known material parameters. In this study, therefore, grain boundaries are allowed to have a finite width and by employing a different gradient plasticity framework, it is possible to obtain the local strain distribution in a nanocrystal. Particularly, the GB is allowed to act as a "strengthener" in the microcrystalline regime and as a "softener" in the nanocrystalline one, providing a unified simple analytical expression that can capture both the "normal" and "abnormal" H–P relation. The underlying idea is that the "bulk" and the "GB" spaces interchange their role to accommodate deformation as the grain size crosses over from the microcrystalline to the nanocrystalline regime. As the scale transitions to nanodimensions, the "bulk" becomes incapable of supporting dislocation nucleation and motion due to its small volume constrained by the relatively thick GB space (and adjacent layers), where most of the dislocation activity occurs, resulting in overall macroscopic plastic deformation.

In the sequel, it will be shown that allowing for this "GB" versus "grain" distinction the mechanical response of nanocrystals below a critical grain size can be captured. Furthermore, by directly relating the present gradient plasticity formulation to that used previously[15,16] allows for the interface energy to be defined as a function of the GB and GI material properties such as the yield stress. The theoretical model will be shown to be in precise agreement with both experimental[1–8] and simulation[18] data for nanomaterials.

It should be noted that in addition to the aforementioned three approaches, other individual models have also been developed to capture the inverse H–P relationship and resulted in the following conclusions: (i) impurity segregation at grain boundaries decreases as the scale decreases, resulting hence in softer boundaries and a softer overall response for nanomaterials below a certain grain size,[19] (ii) the nonequilibrium structure of nanosized grains results in softening,[20] and (iii) the melting temperature decrease of nanomaterials contributes to their hardness decrease.[8]

II. CAPTURING THE INVERSE H–P RELATIONSHIP

As mentioned in the introduction, gradient plasticity has been able to capture to some extent the inverse H–P behavior by allowing for an interface energy term. In this study, an alternative, more physically based model, will be presented that allows explicit consideration of grain boundaries in nanomaterials. In contrast to earlier papers,[15,16] therefore, it is assumed here that the GB does not act as a surface of discontinuity for the plastic strain gradient and its conjugate third-order stress. Instead, it has a finite width $\delta = 2L_{gb}$ and acts as a separate phase constrained by the two adjacent grains. Early experimental evidence[21] has shown that below a critical grain size, deformation occurs through grain rotation and no dislocations form in the purely elastic grains. The GB, hence, in the present framework is assumed to be soft and prone to deformation through rotation/sliding, whereas the GI is purely elastic. In Ref. 22, it was theoretically described that during GB sliding, defects such as GB dislocations and dipoles of wedge disclinations are produced. Such defects are not constrained only into the GB phase, but diffuse to a limited extent into the grain phase, forming therefore a plastic GI–GB layer adjacent to the GB, while the remaining GI core remains purely elastic. The boundary layers, therefore, with thickness L_g, allow for the transition from the ductile GB to the rigid grain core and are considered in the unit cell model of Fig. 1.

Before proceeding with listing the basic equations of the gradient plasticity theory used and its application to the unit cell configuration of Fig. 1, it is remarked that the key physical assumptions of the present model have also been used, in a different context and theoretical framework, by other prominent researchers in the past for deformation at the nanoscale. For example, previous theoretical frameworks[23,24] also assume GB softening to occur due to the underlying mechanism of Coble creep; further information on creep in nanomaterials can be found in Ref. 25 and references therein. GB layers similar to that in Fig. 1 have also been successfully considered,[26,27] while dislocation-based models[28–30] consider that plastic flow occurs predominantly in the GB space network while the GI core remains elastic.

The basic structure of the gradient plasticity theory to be used is summarized below.

A. Gradient plasticity framework

In the strain gradient plasticity framework, both the displacement and plastic strain are the independent kinematic variables.[31] The uniqueness of the solution emerges by finding suitable displacement and plastic strain fields $(u_i, \varepsilon_{ij}^p)$ that minimize the energy functional for the domain Ω under consideration:

$$\Psi(\varepsilon_{ij},\varepsilon_{ij}^p) = \int_\Omega U(\varepsilon_{ij},\varepsilon_{ij}^p,\varepsilon_{ij,k}^p)d\Omega \quad , \qquad (1)$$

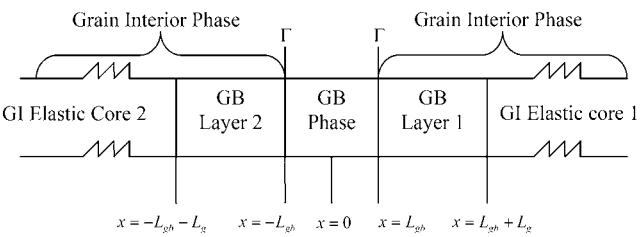


FIG. 1. Unit cell model with grain boundary (GB) phase, grain interior (GI) phase comprised of GI–GB layers, and elastic GI cores.

https://doi.org/10.1557/jmr.2011.123 Published online by Cambridge University Press

where U is the elastoplastic potential energy density and depends on the total strain ε_{ij}, the plastic strain ε^p_{ij}, and the plastic strain gradient $\varepsilon^p_{ij,k}$, as

$$U(\varepsilon_{ij},\varepsilon^p_{ij},\varepsilon^p_{ij,k}) = \frac{1}{2}(\varepsilon_{ij}-\varepsilon^p_{ij})L_{ijkl}(\varepsilon_{ij}-\varepsilon^p_{ij}) + V(\varepsilon^p_{ij},\varepsilon^p_{ij,k}) \quad . \tag{2}$$

The quantity V is the gradient dependent plastic potential, and in the case of classical plasticity, it would not depend on $\varepsilon^p_{ij,k}$. The conjugate variables associated with $(\varepsilon_{ij},\varepsilon^p_{ij},\varepsilon^p_{ij,k})$ are

$$\sigma_{ij} = L_{ijkl}(\varepsilon_{kl}-\varepsilon^p_{kl}),\ \ s_{ij} = -\sigma_{ij} + \frac{\partial V}{\partial \varepsilon^p_{ij}},\ \ \tau_{ijk} = \frac{\partial V}{\partial \varepsilon^p_{ij,k}} \quad . \tag{3}$$

Performing the principal of virtual work and applying the divergence theorem, the governing equilibrium relations in the plastically deformed volume are:

$$\sigma_{ij,j} = 0;\ \ s_{ij} = \tau_{ijk,k} \quad . \tag{4}$$

If the displacement is prescribed, the boundary conditions at the external surface are

$$\tau_{ijk}n_j = 0 \text{ and } u_i = \bar{u}_i \quad . \tag{5}$$

And if one assumes the presence of internal boundaries within the domain Ω, the stress and higher-order stress would be continuous across them as the variational principle gives

$$[\sigma_{ij}n_j] = 0 \text{ and } [\tau_{ijk}n_k] = 0 \text{ across internal boundaries} \quad , \tag{6}$$

where the brackets $[f]$ denote the difference, $f_1 - f_2$, of the enclosed quantity across the interface (the interface normal direction points from "side 2" to "side 1"). Hence, the stress, σ_{ij}, and higher-order stress, τ_{ijk}, are continuous across the boundaries where the GB phase meets with the boundary layer.

When a separate interface energy term, $\varphi(\varepsilon^p_{ij})$, is assigned to grain boundaries, which are collectively denoted as Γ, the energy functional reads[17]

$$\Psi(\varepsilon_{ij},\varepsilon^p_{ij}) = \int_\Omega U(\varepsilon_{ij},\varepsilon^p_{ij},\varepsilon^p_{ij,k})d\Omega + \int_\Gamma \varphi(\varepsilon^p_{ij}) \quad . \tag{7a}$$

By carrying out the principle of virtual work, the same equilibrium and boundary conditions are obtained as before [Eqs. (4) and (5)], but now an interface condition is obtained as

$$[\sigma_{ij}n_j] = 0 \text{ and } [\tau_{ijk}n_k] = \varphi'(\varepsilon^p_{ij}) \quad . \tag{7b}$$

B. Capturing the dependence of grain size on the yield stress

To proceed with analyzing the mechanical response of the one-dimensional configuration of Fig. 1, the plastic potential V must be defined. Since deformation at the nanoscale is not dominated by dislocation motion, strain hardening is not an expected deformation mechanism; instead deformation is taken to be perfectly plastic[13] and, therefore, the plastic potential in the GB phase, and the adjacent to it GB layers, is taken to depend on the plastic strain gradient so as to allow for perfect plasticity after yielding[17]

$$V_{gb} = \sigma^0_{gb}\left|\varepsilon^p_{gb}\right| + \frac{1}{2}\beta_{gb}\ell^2_{gb}\left(\varepsilon^p_{gb,x}\right)^2,$$
$$V_g = \sigma^0_g\left|\varepsilon^p_g\right| + \frac{1}{2}\beta_g\ell^2_g\left(\varepsilon^p_{g,x}\right)^2 \quad , \tag{8}$$

where (β_{gb}, β_g) and (ℓ_{gb}, ℓ_g) denote hardening moduli and internal lengths, respectively, while $\left(\sigma^0_{gb}, \sigma^0_g\right)$ and $\left(\varepsilon^p_{gb}, \varepsilon^p_g\right)$ are the yield stresses and plastic strains of the GB and GB layer respectively; since the GB layer is part of the grain, σ^0_g is equal to yield stress of the grain. Inserting Eq. (8) in Eq. (4) and solving the resulting differential equation gives $\varepsilon^p = -(\bar{\sigma}-\sigma^0_i)x^2/(\beta_i\ell^2_i) + A_i x + B_i$, (i = gb, g), where $\bar{\sigma}$ is the applied stress. The constants of integration A_i and B_i are obtained from the continuity conditions

$$\varepsilon^p_{g1}(L_{gb}+L_g) = 0, \qquad \varepsilon^p_{g1}(L_{gb}) = \varepsilon^p_{gb}(L_{gb}),$$
$$\tau_{g1}(L_{gb}) = \tau_{gb}(L_{gb}),$$
$$\varepsilon^p_{g2}(-L_{gb}-L_g) = 0, \qquad \varepsilon^p_{g2}(-L_{gb}) = \varepsilon^p_{gb}(-L_{gb}),$$
$$\tau_{g2}(-L_{gb}) = \tau_{gb}(-L_{gb}) \quad . \tag{9}$$

Finally, on setting the plastic strain gradient equal to zero at the interface of the GB layer with the elastic core of the GI, i.e., $\varepsilon^p_{,x}\left[\pm(L_{gb}+L_g)\right] = 0$ gives

$$\bar{\sigma} = \frac{L_{gb}\sigma^0_{gb} + L_g\sigma^0_g}{L_{gb}+L_g} \Rightarrow L_g = \frac{\bar{\sigma}-\sigma^0_{gb}}{\sigma^0_g-\bar{\sigma}}L_{gb} \quad . \tag{10}$$

It is interesting to note that Eq. (10) is essentially a statement of the rule of mixtures. On assuming that $\sigma^0_{gb} < \sigma^0_g$, i.e., that the GB phase is softer than the GB layer, Eq. (10) suggests that the thickness of the GB layer increases as the applied stress $\bar{\sigma}$ increases.

Another interesting observation is to compute the difference $\tau(L_{gb}) - \tau(-L_{gb})$. According to Eq. (7) of the approach in Ref. 17, the jump of τ across the GB equals the derivative of the interface energy parameter $\varphi'(\varepsilon^p_{ij})$. By letting $\varphi(\varepsilon^p) = \gamma_{gb}\varepsilon^p$, as in Refs.15 and 16, it is found that

https://doi.org/10.1557/jmr.2011.123 Published online by Cambridge University Press

$$\tau_{gb}(L_{gb}) - \tau_{gb}(-L_{gb}) = -\frac{2L_g L_{gb}\left(\sigma_g^0 - \sigma_{gb}^0\right)}{L_{gb} + L_g} = \gamma_{gb} \Rightarrow \sigma_{gb}^0 = \sigma_g^0 + \frac{L_{gb} + L_g}{2L_g L_{gb}}\gamma_{gb} \quad . \tag{11}$$

Equation (11) illustrates how the interface energy model[17] can be related to the present multiphase model, which by allowing for grain boundaries to have a finite thickness, it derives a microscopic expression for the interface energy parameter γ_{gb}. It should be noted that, according to Eq. (11), γ_{gb} is positive as the grain boundaries inhibit plastic flow ($\sigma_{gb}^0 > \sigma_g^0$), whereas at the nano regime, γ_{gb} is negative as the grain boundaries become the carriers of plastic deformation and are softer than the GI ($\sigma_{gb}^0 < \sigma_g^0$).

Upon insertion of Eq. (11) into Eq. (10), we obtain

$$\bar{\sigma} = \sigma_g^0 + \frac{\gamma_{gb}}{2L_g} \quad . \tag{12}$$

Since σ_g^0 is the yield stress of the grain, it can be allowed to follow the standard H–P relation, i.e., $\sigma_g^0 = \sigma_0 + k/\sqrt{d}$ and allowing the boundary layer thickness to be a fraction of the grain size d, i.e., $L_g = ad$ with $0 < a < 1$, Eq. (12) yields

$$\bar{\sigma} = \sigma_0 + \frac{k}{\sqrt{d}} + \frac{\gamma_{gb}}{2ad} \quad . \tag{13}$$

Equation (13) gives the stress of the unit cell depicted in Fig. 1 upon yielding of the GB and boundary layers; it, therefore, corresponds to the yield stress of the nanocrystal, and it is used to fit experimental data obtained for seven different nanocrystalline materials, which exhibit both normal and abnormal H–P behavior. In particular, such experimental data exist for Cu,[1] Fe-Mo-Si-B alloy,[2] Ni-Al alloy,[3] Zn,[4] WC-NiAl,[5] Pd,[6,8] and $Ni_{20}P_{80}$ alloy.[7,8] Although the fabrication methods for each nanocrystal differ, in all cases[1–8] their hardness was reported, and according to Tabor's rule (*hardness*/3 = σ_0),[32] it was converted into the yield stress so as to directly fit Eq. (13) to these data. The corresponding values of the parameters are given in Table I. A similar expression to that in Eq. (12) was obtained by the interface gradient plasticity model,[15,16] but the underlying physical mechanisms were not elaborated as they are here.

Furthermore, it is noted that the critical grain size d_c where the transition from the "normal" to the "abnormal" H–P behavior occurs can be determined from Eq. (13) by setting $\partial\bar{\sigma}/\partial d = 0$, giving

$$d_c = (\gamma_{gb}/(ak))^2 \quad . \tag{14}$$

TABLE I. Values of the parameters used to generate the fits in Fig. 2.

	K(kPa$\sqrt{m}$)	σ_0 (MPa)	A	$-\gamma_{gb}$ (N/m)
Cu	124	28	0.01	0.225
Fe-Mo-Si-B alloy	1010	380	0.01	1.74
Ni-Al alloy	1190	262	0.01	1.61
Zn	55	30	0.01	0.05
WC-NiAl	1460	300	0.01	1.59
Pd	261	50	0.01	0.32
$Ni_{20}P_{80}$ alloy	197	1080	0.01	0.162

It should be noted that the values for the parameters in Table I cannot be compared with previous experimental data, since all existing data in the literature are for bulk or single crystal materials, not for nanocrystalline as in the present case.

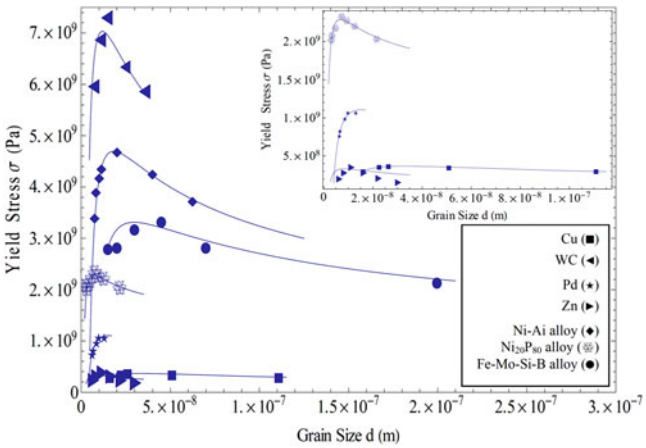


FIG. 2. Fitting of experimental data to theory.

Equation (14) can be thought of as the micro-to-nano scale transition criterion as it defines that the critical grain size at which material behavior "switches" from micron to nano can be directly computed if the GB energy (γ_{gb}), the fraction of the GB thickness that yields (a), and the H–P slope (k) are known. Furthermore, inserting Eq. (14) in Eq. (13) provides the peak strength observed in crystalline materials. Although similar analytical expressions that can predict this transition do not exist, it was proposed in Ref. 33 that the peak strength of nanomaterials is reached when the strain rate contribution from the GB shear is equal to the alternative contribution from dislocation plasticity inside the grain.

III. PREDICTING SIZE EFFECTS IN THE FLOW STRESS WHEN $d < d_c$

Having successfully interpreted the softening that occurs in the yield stress of nanocrystals as the grain size decreases, it is of interest to try and model the softening that takes place in the flow stress of such materials. Atomistic simulations[18] have shown that decreasing the grain size of nanocrystalline Cu below a critical value results in a softening in the flow stress required for continuous

https://doi.org/10.1557/jmr.2011.123 Published online by Cambridge University Press

deformation. This was attributed[18] to the fact that plastic deformation initiated and was carried out in the grain boundaries while the grains remained mostly elastic. Since these statements are in agreement with the assumptions made in the aforementioned theoretical model, it is of interest to use this theoretical approach to capture the full stress–strain simulation curves that have been obtained for nanopolycrystalline Cu with varying grain size d ($d < d_c$). To this end, we relax the geometric configuration of the unit cell model of Fig. 1 by neglecting the details associated with the GB layers, as shown in Fig. 3.

As mentioned in the previous section, it is assumed that for the nanoscale $\sigma_{gb}^0 < \sigma_g^0$. From a theoretical point of view, deformation is taken to occur in the following stages: (i) initially the whole material deforms elastically, (ii) after the initial elastic deformation, the GB will yield providing a knee in the stress–strain curve. GB yielding is assumed to occur due to sliding, rotation, and diffusion, as mentioned in the introduction. (iii) If deformation is sufficient, the GI phase will also yield at a critical load and a strain burst will occur (in Ref. 18, it is stated that some plastic deformation occurs in the grains). It should be noted that upon grain yielding, deformation will become perfectly plastic since it has been observed that deformation in grains at the nanoscale occurs through shear band formation, which corresponds to perfect plasticity.[13] (iv) Finally, increasing further the applied load, it is possible for some hardening to take place, after this perfectly plastic response, however, the simulations did not extend to such loads and rehardening after perfect plasticity did not occur.

In Ref. 34, the stress–strain responses for each of the aforementioned deformation stages were found, using the previously described gradient plasticity framework, Eqs. (1)–(6), but the plastic potential V was taken to be $V_i(\varepsilon_i^p, \varepsilon_{i,x}^p) = \sigma_i^0 |\varepsilon_i^p| + \frac{1}{2}\beta_i \left[(\varepsilon_i^p)^2 + \ell_i^2 \left(\varepsilon_{i,x}^p\right)^2 \right]$. In particular, during the initial elastic deformation the stress–strain relationship was found as

$$\bar{\sigma} = \frac{E_g E_{gb}\left(L_g + L_{gb}\right)}{E_g L_{gb} + E_{gb} L_g}\bar{\varepsilon} \quad , \tag{15}$$

where (E_g, E_{gb}) denote the elastic moduli, $\bar{\varepsilon}$ is the total strain and $L = L_g + L_{gb}$. After the GB phase yielded, a "knee" is observed in the stress–strain plot and the stress was given as

$$\bar{\sigma} = \frac{\beta_{gb} E_g E_{gb}\left(L_g + L_{gb}\right)\bar{\varepsilon} + E_g E_{gb}\left(L_{gb} - \ell_{gb}\tanh\left(\ell_{gb}^*\right)\right)\sigma_{gb}^0}{\beta_{gb}\left(E_g L_{gb} + E_{gb} L_g\right) + E_g E_{gb}\left(L_{gb} - \ell_{gb}\tanh\left(\ell_{gb}^*\right)\right)} \quad , \tag{16}$$

where $\ell_i^* = L_i/\ell_i$. With continuous deformation, the GI also began to deform in a perfectly plastic manner, through shear band formation,[13] when the strain was equal to

$$\bar{\varepsilon}_g^{\triangleleft} = \left(\frac{f_{gb}}{E_{gb}} + \frac{f_g}{E_g}\right)\sigma_{gb}^0 + \left(\frac{f_{gb}}{E_{gb}} + \frac{f_g}{E_g} + \frac{f_{gb}}{\beta_{gb}} - \frac{1}{\beta_{gb}}\frac{\ell_{gb}}{L}\tanh\left(\ell_{gb}^*\right)\right) \times \left(\sigma_g^0 - \sigma_{gb}^0\right) \quad , \tag{17}$$

where $f_i = L_i/L$. Finally, for sufficient high deformation, re-hardening could occur after the grain yielded, according to

$$\bar{\sigma} = \sigma_g^0 + \left\{ \frac{\beta_{gb}\beta_g(L_{gb}E_g + L_g E_{gb}) + E_{gb}E_g(L_{gb}\beta_g + L_g\beta_{gb})}{\beta_{gb}\beta_g E_{gb} E_g L} + \frac{1}{L} \times \left(\frac{1}{\beta_{gb}} - \frac{1}{\beta_g}\right) \frac{(\beta_{gb} - \beta_g)\ell_{gb}\ell_g \tanh\left(\ell_{gb}^*\right)\tanh\left(\ell_g^*\right)}{\left(\beta_{gb}\ell_{gb}\tanh\left(\ell_{gb}^*\right) + \beta_g \ell_g \tanh\left(\ell_g^*\right)\right)} \right\}^{-1} \times \left(\bar{\varepsilon} - \bar{\varepsilon}_g^{\triangleright}\right) \quad , \tag{18}$$

with $\bar{\varepsilon}_g^{\triangleright}$ representing the starting strain of GI hardening

$$\bar{\varepsilon}_g^{\triangleright} = \left(\frac{f_{gb}}{E_{gb}} + \frac{f_g}{E_g}\right)\sigma_{gb}^0 + \left[\frac{f_{gb}}{E_{gb}} + \frac{f_g}{E_g} + \frac{f_{gb}}{\beta_{gb}} + \frac{\left(\beta_{gb} - \beta_g\right)\ell_{gb}\ell_g \tanh\left(\ell_{gb}^*\right)\tanh\left(\ell_g^*\right)}{\beta_{gb} L\left(\beta_{gb}\ell_{gb}\tanh\left(\ell_{gb}^*\right) + \beta_g \ell_g \tanh\left(\ell_g^*\right)\right)} \times \left(\sigma_g^0 - \sigma_{gb}^0\right)\right] \quad . \tag{19}$$

The difference of the strain before and after the strain burst will give the magnitude of the plateau, indicating perfect plasticity, as

$$\Delta\bar{\varepsilon} = \bar{\varepsilon}_g^{\triangleright} - \bar{\varepsilon}_g^{\triangleleft} = \frac{\ell_{gb}\tanh\left(\ell_{gb}^*\right)}{L_g + L_{gb}} \frac{\ell_g \tanh\left(\ell_g^*\right) + \ell_{gb}\tanh\left(\ell_{gb}^*\right)}{\beta_{gb}\ell_{gb}\tanh\left(\ell_{gb}^*\right) + \beta_{gb}\ell_{gb}\tanh\left(\ell_{gb}^*\right)} \times \left(\sigma_g^0 - \sigma_{gb}^0\right) \quad . \tag{20}$$

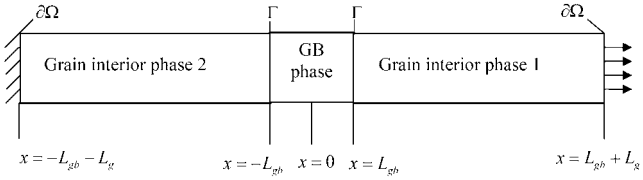


FIG. 3. Geometric configuration of the unit cell model, consisting of a GB phase and a GI phase, for predicting size-dependent stress–strain curves.

https://doi.org/10.1557/jmr.2011.123 Published online by Cambridge University Press

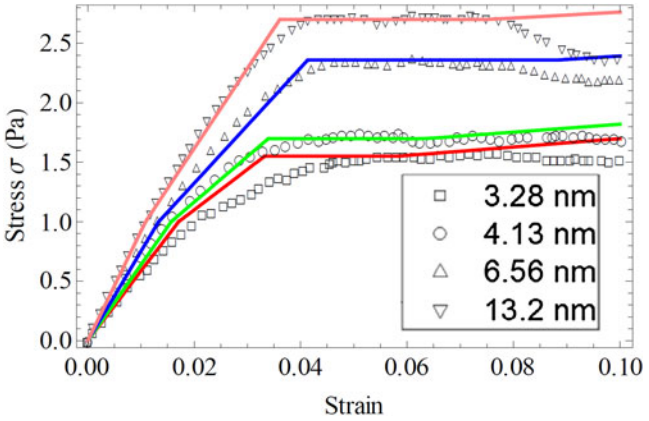


FIG. 4. Fit of theoretical model to MD simulations.[18]

TABLE II. The fitting parameters for Fig .4.

	L_g = 3.28 nm	L_g = 4.13 nm	L_g = 6.56 nm	L_g = 13.2 nm	
σ^0_{gb}(GPa)	1	1	1	1	
σ^0_g(GPa)	1.55	1.70	2.36	2.70	
E_g (GPa)	E_{gb} (GPa)	L_{gb} (nm)	ℓ_{gb} (nm)	β_{gb} (GPa)	β_g (GPa)
127	27	1.5	1	10	2

The aforementioned stress–strain curves have been plotted qualitatively,[34] but no comparison was performed with simulation data[18]; here however, the above equations are directly fit to stress–strain curves[18] in Fig. 4. It can be seen that in the simulations there is no strain hardening stage after the plateau due to the computational cost. The material parameters that were chosen here, therefore, (Table II) allow for a large strain burst during grain yielding and minimal hardening after the burst, to fit the simulation profile. The fits obtained are indeed in agreement with,[18] and it should be noted that is the first time that a continuum theoretical model can capture this behavior. Finally, it can be noted that the same plasticity mechanisms of GB sliding were used to predict the flow stress in nanocrystalline Cu when the grain size was 10 nm.[22] It would be interesting to use the model of[22] with varying grain sizes and see if similar size effects as those of Fig. 4 are obtained.

IV. CONCLUSIONS

It was illustrated that gradient plasticity can be conveniently used to interpret GB hardening and softening as the grain size crosses over from the micrometer to the nanometer regime, by allowing grain boundaries to have a finite thickness, and a lower yield stress from the grains. In particular, an analytical expression is obtained for the critical grain size at which the "micro" to "nano" transition in deformation mechanisms occurs, and very good fits are performed to experimental data for the hardness dependence on the grain size. Furthermore, it is shown for the first time that gradient plasticity can effectively capture the softening in the flow stress of nanocrystalline Cu that has been observed in atomistic simulations.[18]

ACKNOWLEDGMENT

The authors are grateful to KEA's European Research Council Starting Grant MINATRAN 211166 for its support.

REFERENCES

1. P.G. Sanders, J.A. Eastman, and J.R. Weertman: Elastic and tensile behavior of nanocrystalline copper and palladium. *Acta Mater.* **45**, 4019 (1997).
2. X.D. Liu, Z.Q. Hu, and B.Z. Ding: Hall-Petch relation in nanocrystalline Fe-Mo-Si-B alloys. *Nanostruct. Mater.* **2**, 545 (1993).
3. T. Volpp, E. Göring, W.M. Kuschke, and E. Arzt: Grain size determination and limits to Hall-Petch behavior in nanocrystalline NiAl powders. *Nanostruct. Mater.* **8**, 855 (1997).
4. J. Narayan, R.K. Venkatesan, and A. Kvit: Structure and properties of nanocrystalline zinc films. *J. Nanopart. Res.* **4**, 265 (2002).
5. R. Venkatesan, A. Kvit, Q. Wei, and J. Narayan: Novel tungsten carbide nanocrystalline composites by pulsed laser deposition, in *Structure and Mechanical Properties of Nanophase Materials—Theory and Computer Simulations vs. Experiment*, edited by D. Farkas, H. Kung, M. Mayo, H. Van Swygenhoven, and J. Weertman (Mater. Res. Soc. Symp. Proc. **634**, Warrendale, PA, 2000), B6.1.1.
6. A.H. Chokshi, A. Rosen, J. Karch, and H. Gleiter: On the validity of the Hall-Petch relationship in nanocrystalline materials. *Scr. Metall.* **23**, 1679 (1989).
7. G. Palumbo, U. Erb, and K.T. Aust: Triple line disclination effects on the mechanical behaviour of materials. *Scr. Metall. Mater.* **24**, 2347 (1990).
8. M. Zhao, J.C. Li, and Q. Jiang: Hall–Petch relationship in nanometer-size range. *J. Alloy. Comp.* **361**, 160 (2003).
9. L. Lu, X. Chen, X. Huang, and K. Lu: Revealing the maximum strength in nanotwinned copper. *Science* **323**, 607 (2009).
10. M. Meyers, A. Mishra, and D. Benson: Mechanical properties of nanocrystalline materials. *Prog. Mater. Sci.* **51**, 427 (2006).
11. C.S. Pande and K.P. Cooper: Nanomechanics of Hall–Petch relationship in nanocrystalline materials. *Prog. Mater. Sci.* **54**, 689 (2009).
12. G. Saada and G. Dirras: Chapter 90 Mechanical properties of nanograined metallic polycrystals, in *Dislocations in Solids Volume 15*, edited by J.P. Hirth and L. Kubin (Elsevier, Amsterdam, 2009), p. 199.
13. J.E. Carsley, J. Ning, W.W. Milligan, S.A. Hackney, and E.C. Aifantis: A simple, mixtures-based model for the grain size dependence of strength in nanophase metals. *Nanostruct. Mater.* **5**, 441 (1995).
14. D.A. Konstantinidis and E.C. Aifantis: On the "anomalous" hardness of nanocrystalline materials. *Nanostruct. Mater.* **10**, 1111 (1998).
15. K.E. Aifantis and A.A. Konstantinidis: Hall–Petch revisited at the nanoscale. *Mater. Sci. Eng., B* **163**, 139 (2009).
16. K.E. Aifantis and A.A. Konstantinidis: Yielding and tensile behavior of nanocrystalline copper. *Mater. Sci. Eng., A* **503**, 198 (2009).

https://doi.org/10.1557/jmr.2011.123 Published online by Cambridge University Press

17. K.E. Aifantis and J.R. Willis: The role of interfaces in enhancing the yield strength of composites and polycrystals. *J. Mech. Phys. Solids* **53**, 1047 (2005).
18. J. Schiotz, T. Vegge, F.D. Di Tolla, and K.W. Jacobsen: Atomic-scale simulations of the mechanical deformation of nanocrystalline metals. *Phys. Rev. B* **60**, 11971 (1999).
19. J.C.M. Li: Grain boundary impurity and porosity effects on the yield strength of nanocrystalline materials. *Appl. Phys. Lett.* **90**, 041912 (2007).
20. R.W. Armstrong, H. Conrad, and F.R.N. Nabarro: Meso-to-nanoscopic polycrystal/composite strengthening, in *Mechanical Properties of Nanostructured Materials and Nanocomposites*, edited by I. Ovid'ko, C.S. Pande, R. Krishnamoorti, E. Lavernia, and G. Skandan (Mater. Res. Soc. Symp. Proc. **791**, Warrendale, PA, 2004), p. 69.
21. M. Ke, S.A. Hackney, W.W. Milligan, and E.C. Aifantis: Observation and measurement of grain rotation and plastic strain in nanostructured metal thin films. *Nanostruct. Mater.* **5**, 689 (1995).
22. I.A. Ovid'ko and A.G. Sheinerman: Enhanced ductility of nanomaterials through optimization of grain boundary sliding and diffusion processes. *Acta Mater.* **57**, 2217 (2009).
23. H.S. Kim, Y. Estrin, and M.B. Bush: Constitutive modelling of strength and plasticity of nanocrystalline metallic materials. *Mater. Sci. Eng., A* **316**, 195 (2001).
24. H.S. Kim, Y. Estrin, and M.B. Bush: Plastic deformation behaviour of fine-grained materials. *Acta Mater.* **48**, 493 (2000).
25. R.W. Armstrong: Plasticity: Grain size effects II, in *Encyclopedia of Materials: Science and Technology*, edited by K.H.J. Buschow, W.C. Robert, C.F. Merton, I. Bernard, J.K. Edward, M. Subhash, and V. Patrick (Elsevier, Oxford, England, 2005), p. 1.
26. H.H. Fu, D.J. Benson, and M.A. Meyers: Analytical and computational description of effect of grain size on yield stress of metals. *Acta Mater.* **49**, 2567 (2001).
27. M.A. Meyers and E. Ashworth: A model for the effect of grain size on the yield stress of metals. *Philos. Mag. A* **46**, 737 (1982).
28. M.Y. Gutkin, I.A. Ovid'ko, and N.V. Skiba: Strengthening and softening mechanisms in nanocrystalline materials under superplastic deformation. *Acta Mater.* **52**, 1711 (2004).
29. I.A. Ovid'ko: Superplasticity and ductility of superstrong nanomaterials. *Rev. Adv. Mater. Sci.* **10**, 89 (2005).
30. K.A. Padmanabhan and H. Gleiter: Optimal structural superplasticity in metals and ceramics of microcrystalline- and nanocrystalline-grain sizes. *Mater. Sci. Eng., A* **381**, 28 (2004).
31. K. Aifantis and A. Ngan: Modeling dislocation—grain boundary interactions through gradient plasticity and nanoindentation. *Mater. Sci. Eng., A* **459**, 251 (2007).
32. D. Tabor: *The Hardness of Metals* (Oxford University Press, 2000).
33. A.S. Argon and S. Yip: The strongest size. *Philos. Mag. Lett.* **86**, 713 (2006).
34. X. Zhang and K.E. Aifantis: Accounting for grain boundary thickness in the sub-micron and nano scales. *Rev. Adv. Mater. Sci.* **26**, 74 (2010).
35. E.C. Aifantis: On the microstructural origin of certain inelastic models. *Trans. ASME, J. Eng. Mat. Techn.* **106**, 326 (1984).

https://doi.org/10.1557/jmr.2011.123 Published online by Cambridge University Press